International Journal of Thermophysics, Vol. 21, No. 2, 2000

Effective Thermal Conductivity and Permeability of Aluminum Foam Materials[1]

J. W. Paek,[2] B. H. Kang,[2,4] S. Y. Kim,[2] and J. M. Hyun[3]

An experimental measurement program was performed to determine thermophysical properties of aluminum-based foam metals. The effective thermal conductivity k_e and permeability K were investigated in detail. Experimental facilities were fabricated, and the measurement procedures and methodologies were evaluated. One-dimensional heat conduction was considered to determine k_e. The results indicate that k_e increases as the porosity ε decreases. However, no noticeable changes in k_e were detected from variations of the cell size of the foam metal at a fixed porosity ε. The permeability K is substantially affected by both ε and the cell size. An empirical correlation for the friction factor f is proposed based on the concepts of K and inertial effect.

KEY WORDS: aluminum foam metal; effective thermal conductivity; friction factor; permeability; pressure loss.

1. INTRODUCTION

The use of porous media is widespread in industrial applications. The main advantage is the high surface-area-to-volume ratio, which leads to enhanced heat transport and miniaturization of thermal systems. One eminent example is a packed bed, which is frequently utilized in catalytic converters and thermal energy storage devices [1, 2]. One drawback of a packed bed is

[1] Paper presented at the Fifth Asian Thermophysical Properties Conference, August 30–September 2, 1998, Seoul, Korea.

[2] Thermal/Flow Control Research Center, Korea Institute of Science and Technology, Seoul 136-791, Korea.

[3] Department of Mechanical Engineering, Korea Advanced Institute of Science and Technology, Taejon 305-701, Korea.

[4] To whom correspondence should be addressed.

0195-928X/00/0300-0453$18.00/0

that it incurs a large pressure drop for the throughflow, since the packed bed, as a whole, is a dense material of porosity ε, which implies a void fraction in the material in the range of 0.3–0.6. In addition, the particles in a packed bed normally have localized points of contact; therefore, the effective thermal conductivity of the system is generally low [3, 4].

Foam material has been introduced recently to remedy some of the above shortcomings. Foam material is a highly permeable porous medium with high porosity, typically $\varepsilon \geqslant 0.9$, which enables a considerably reduced pressure drop for the throughflow. Also, the solid ligaments in foam material make directly connected contacts which increase the effective thermal conductivity of the entire system. As the base substance of a foam material, aluminum has emerged as a strong candidate because of its low mass density and high thermal conductivity. The attractiveness of aluminum-based foam material is being considered for practical heat-transfer enhancement technologies [5, 6]. In view of these industrial developments, it is important to establish detailed methodologies and procedures for determining the important thermophysical properties of a specific foam metal. In particular, knowledge of the effective thermal conductivity and the physical factors, including permeability, involved in pressure drop is essential for successful design and operation of high-performance thermal systems.

The physicochemical structures of foam metal are very complex and irregular, which virtually rules out the possibility of analytical approaches [6–8]. The parameters affecting the thermophysical properties of foam metal include the conductivities of solid and fluid, porosities, geometrical parameters, etc. Most research studies have therefore been directed at experimental measurements; however, published accounts on this subject are scarce, and the scope and depth of prior experiments have been limited. Moreover, the measurement data available in the literature on the pressure drop in a foam metal seem to be at variance with each other [5, 9–11]. For the case of a packed bed, similar data on the pressure drop are substantially mutually consistent. These difficulties clearly call for more focused and refined measurement programs to evaluate the principal thermophysical characteristics of foam metal. The present study addresses these concerns.

The aim of the present work is to identify the significant dynamic elements which have strong influence on the thermal conductivity and the permeability of a foam metal. Systematic measurements reveal the relevance of the porosity and cell size of the foam metal under investigation. Empirical correlations are provided for the pressure loss and effective thermal conductivity of an aluminum-based foam metal. Features of the foam metal are suggested which would produce maximal heat transfer and minimal pressure drop throughout the system.

2. EXPERIMENTAL ARRANGEMENT

First we outline the procedures for measuring the thermal conductivity of the foam metal. A special-purpose experimental apparatus, shown in Fig. 1, was fabricated. A one-dimensional, steady-state heat transport is established by maintaining a temperature difference across a layer of the foam metal and a SUS (stainless steel 304) plate layer. Under the assumption that the heat flux is the same in both layers, the effective thermal conductivity of the foam metal can be determined by using the imposed temperature difference and the known value of thermal conductivity ($k_{sus} = 14.9\ \mathrm{W \cdot m^{-1} \cdot K^{-1}}$) of the SUS plate. This method has been employed by various investigators [3, 4, 8].

The steady temperature gradient is created by employing two baths of different constant temperatures. The flat contact surfaces of these baths are established by 10-mm-thick copper plates. The temperature of the bath is maintained by circulating water from an individual thermal reservoir. The temperatures of the hot upper and cold bottom baths are regulated at $50.0 \pm 0.2°C$ and $8.4 \pm 0.1°C$, respectively, by means of an electric heater and a high-precision controller.

The size of the specimen of the foam metal was $90 \times 190 \times 9.1$ mm in width, length, and thickness, respectively, and that of the SUS metal was $90 \times 190 \times 14$ mm. The hot and cold baths are mechanically attached to the top surface of the foam metal and the bottom surface of the SUS plate, respectively. A heat-sink compound was applied to the surfaces to minimize thermal contact resistance. The side walls were wrapped with thick styrofoam insulating layers. Fifteen thermocouples were inserted in the 0.5-mm-deep grooves which were milled on the surfaces of foam metal and SUS plate, as shown in Fig. 1. The junction of the thermocouple was 0.3 mm in

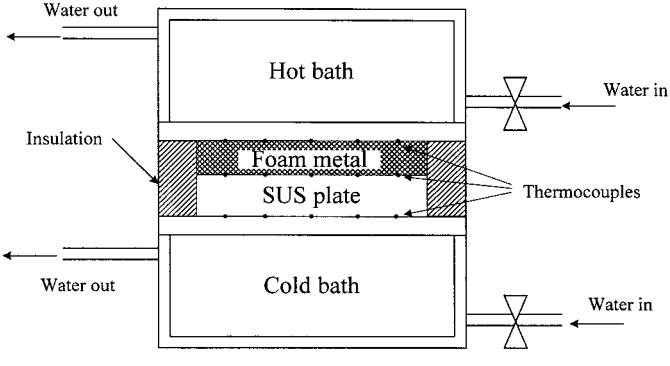

Fig. 1. A schematic diagram of an experimental apparatus for the measurement of effective thermal conductivity.

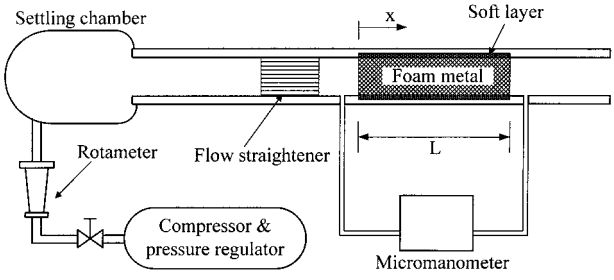

Fig. 2. An experimental apparatus for the measurement of permeability.

diameter. The temperature measurements were carried out by employing T-type thermocouples (AWG 36) and the data logger DR 232 with a resolution of 0.1°C.

The experimental facilities for measuring the permeability of the foam metal are shown in Fig. 2. Since the permeability is closely related to the static pressure (P) drop of throughflow, the static pressure difference between the inlet and exit of the test section was measured. The identical specimen of the foam metal was placed in the test section. The throughflow was supplied by a compressor and regulated by using a fine-precision rotameter. Before entering the test section, the throughflow passes a settling chamber and a flow straightener to obtain a well-controlled uniform stream. The specimen was covered by a thin, soft, cushion-like layer which acts as a buffer between the foam metal and the acrylic wall of the test section. The cushion layer makes a pliant clutch with the irregular surfaces of both the foam metal and the acrylic wall, and this tends to minimize flow leakage through the gap between the foam metal and the wall boundary. The pressure drop is monitored by using a micromanometer (Dwyer's microtector) with a resolution of 10 μm in water head. A conventional inclined manometer was also employed as a backup device.

3. RESULTS AND DISCUSSION

Before proceeding further, it is important to describe the interior geometrical shape of the foam metal. The foam metal in the present study is made of aluminum alloy 6101, of density and thermal conductivity 2690 $kg \cdot m^{-3}$ and 218 $W \cdot m^{-1} \cdot K^{-1}$, respectively. As illustrated in Fig. 3, the diameter d of a cell is the key parameter to characterize the physicochemical properties of a foam metal. In the present study, three cell sizes with $d = 0.65$, 1.25, and 2.50 mm are selected for detailed examination. Since the mass of air in the foam metal is negligibly small compared with

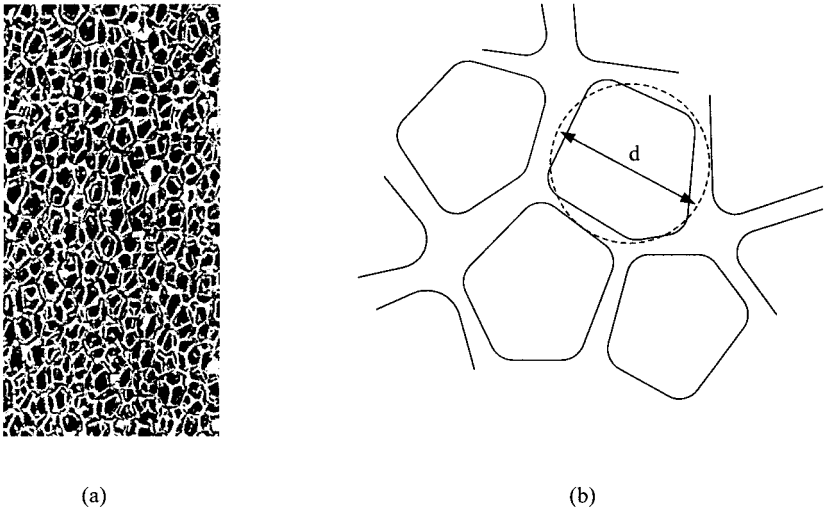

Fig. 3. Structure of the aluminum foam metal in the present study. (a) Aluminum foam metal. (b) Schematic diagram of cell structure.

the mass of the solid structure, the mass of the foam metal is almost the same as that of the solid structure. Therefore, the ratio of the density of the foam metal to the density of the aluminum alloy implies $(1-\varepsilon)$ of the foam metal. The porosities of the foam metal that were measured in the present study were $\varepsilon = 0.89$ to 0.96.

The effective thermal conductivity k_e of the foam metal can be determined by using

$$k_e \frac{\Delta T_{fm}}{H_{fm}} = k_{sus} \frac{\Delta T_{sus}}{H_{sus}} \tag{1}$$

from which

$$k_e = k_{sus} \frac{\Delta T_{sus}}{\Delta T_{fm}} \frac{H_{fm}}{H_{sus}} \tag{2}$$

In the above, H_{sus} and H_{fm} denote, respectively, the thickness of the SUS plate and the foam metal specimen, and ΔT_{sus} and ΔT_{fm} the temperature difference across the SUS plate and the specimen, respectively. The measured temperatures on each surface are ensured to be independent of the compression force of the hot bath. The uncertainty in k_e is attributed mainly to the nonuniform distributions of surface temperatures which may result from misalignments of the thermocouples and solid ligaments. Therefore,

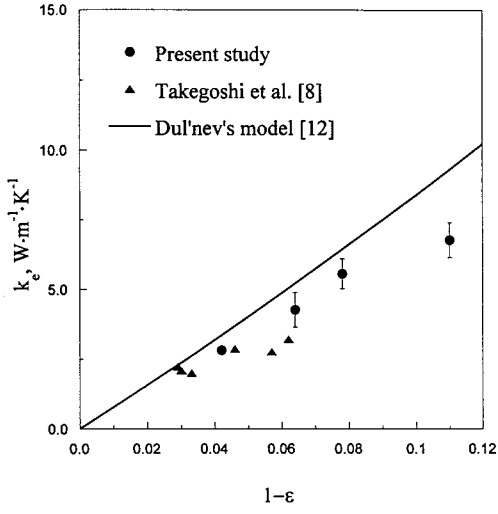

Fig. 4. Effect of porosity on the effective thermal conductivity at a fixed cell size, $d = 1.25$ mm.

the uncertainty increases as the cell size d increases. For the case of $d = 1.25$ mm, the uncertainty in k_e is estimated to be 12%. For an actual data run, the lengthwise averaged values are taken as the quantities of Eq. (2).

The effect of the porosity ε on the effective thermal conductivity k_e is illustrated in Fig. 4 for the case of $d = 1.25$ mm. Obviously, k_e increases as ε decreases, which is intuitively clear. The present data are consistent with the earlier results of Takegoshi et al. [8], which covered a range of relatively high values of ε. The present measurements encompass a broader range of ε, extending the findings of Takegoshi et al. [8]. The general trend of the k_e versus ε relationship was proposed by Dul'nev [12] in qualitative terms by considering simple one-dimensional heat conduction through a unit cubic cell.

In Dul'nev's model, as shown in Fig. 5, the dimensionless thickness t of the solid ligament in the unit cell can be found from

$$t = \frac{1}{2} + \cos\left(\frac{1}{3}\cos^{-1}(2\varepsilon - 1) + \frac{4\pi}{3}\right) \tag{3}$$

Under the assumptions of one-dimensional heat conduction through the cell without convective and radiative heat transfer in the void, the effective thermal conductivity of the foam metal can be represented as

$$k_e = k_s t^2 + k_f (1-t)^2 + \frac{2t(1-t)\, k_f k_s}{k_s(1-t) + k_f t} \tag{4}$$

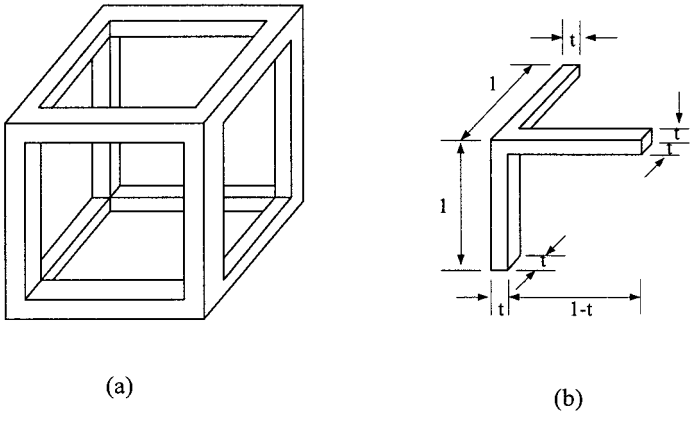

Fig. 5. Dul'nev's model for the effective thermal conductivity of the foam metal. (a) Dul'nev's cubic cell model. (b) Dul'nev's model rearranged for calculating the effective thermal conductivity.

In the above, k_s and k_f are the thermal conductivities of the solid (aluminum alloy 6101) and fluid (air), respectively.

It was ascertained that an increase in porosity is linked to a decrease in the ligament thickness and an increase of void fraction in a given unit cell. However, the increase in heat conduction through the enlarged cross section of the solid ligament far overweighs the decrease in heat conduction

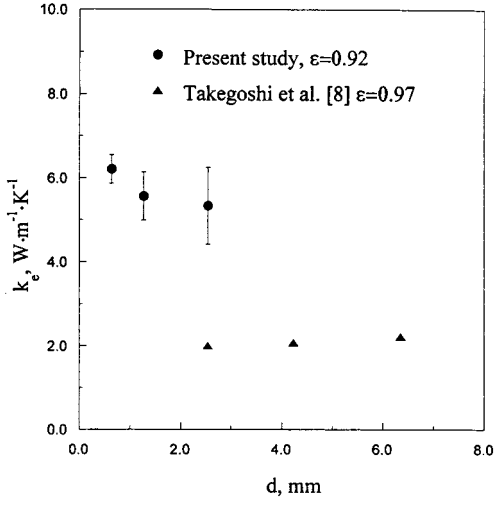

Fig. 6. Effect of cell size on the effective thermal conductivity at a fixed porosity.

through air in the reduced void fraction. This physical reasoning turns up in the linear k_e–ε relation, as proposed by Dul'nev [12], which is plotted in Fig. 4 for comparison purposes.

The measurement results for three different cell sizes ($d = 0.65$–2.50 mm) in Fig. 6 indicate that the effect of the cell size d on the effective thermal conductivity k_e is very small. This is in agreement with the results of Takegoshi et al. [8] for relatively high values of porosity ε. Furthermore, the approximate model of Dul'nev [12] asserts that the impact of d on the determination of k_e is minor. In summary, the primary factor which influences k_e is the porosity ε, and the present efforts over wider ranges of ε and d are consistent with the previous investigations.

Next, measurements of the pressure drop in the x direction are considered. Figure 7 displays variations of the measured pressure loss per unit length of the foam metal versus the velocity of throughflow V at a given porosity ($\varepsilon = 0.92$), i.e., when the cross-sectional area for the passage of throughflow remains unchanged. As the cell size d of a foam metal decreases, the surface-area-to-volume ratio increases, and this means additional flow resistance, which results in an increased pressure drop. The repeatability error for the measurement of pressure drop is estimated to be less than 3%.

The effect of porosity ε on the pressure drop is plotted in Fig. 8 for the case of $d = 1.25$ mm. Pressure drops of various foam metals were normalized by those at $\varepsilon \cong 0.94$. By the normalization, it is evident that both

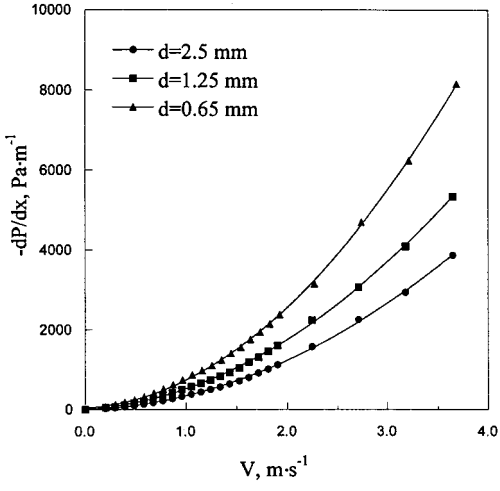

Fig. 7. Effect of cell size on pressure drop at a fixed porosity, $\varepsilon = 0.92$.

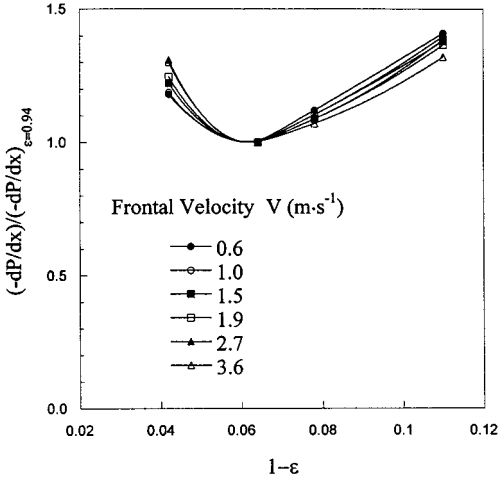

Fig. 8. Normalized pressure drop vs. porosity variations at a fixed cell size, $d = 1.25$ mm.

the porosity and velocity of throughflow have appreciable impacts on the pressure drop. It is noted that the pressure drop becomes minimal around $\varepsilon \cong 0.94$. This can be explained by noting that the pressure drop is substantially influenced by the void fraction as well as the shape of the cell of the foam metal. The above observation is of interest in light of the preceding assertion that k_e is determined principally by ε rather than by the size or shape of the cell. Extending this empirically constructed representation of Fig. 7 leads to an expression

$$-\frac{dP}{dx} = \frac{\mu}{K} V + \frac{\rho C_E}{\sqrt{K}} V^2 \tag{5}$$

which, after rearrangement, can be written as

$$\left(-\frac{dP}{dx}\right)\frac{1}{\mu V} = \frac{1}{K} + \frac{\rho C_E}{\mu \sqrt{K}} V \tag{6}$$

In the above, K and C_E denote, respectively, the permeability and Ergun's coefficient [13]. ρ and μ are the density and dynamic viscosity of air, respectively. The quadratic curve fit shown in Fig. 7 allows the determination of K and C_E. Obviously, K, with the dimension of area, indicates the flow conductance, and C_E accounts for the inertial effect, which becomes meaningful in the high-velocity range.

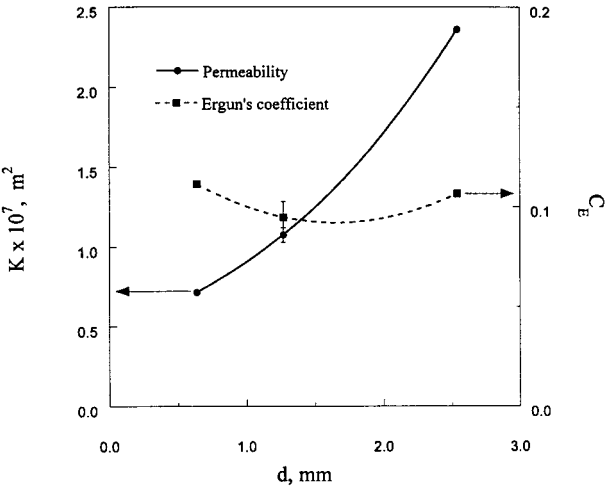

Fig. 9. Effect of cell size on permeability and Ergun's coefficient at a fixed porosity, $\varepsilon = 0.92$.

As it is discernible in the physical meaning of permeability, the permeability K increases as the cell size d increases for fixed porosity ε, as exemplified in Fig. 9. For this particular set of parameters, the changes in C_E are small.

The influence of the porosity ε on the permeability K and Ergun's coefficient C_E is illustrated in Fig. 10. The above described minimal value of pressure drop around $\varepsilon \cong 0.94$ is apparent. In general, the increase in ε gives rise to a wider area for flow passage at a given cell size, which results in a higher value of K.

By recognizing the significance of $\sqrt{K}$ as the permeability-related length scale, the properly defined Reynolds number Re_K and friction factor f are introduced:

$$\mathrm{Re}_K = \frac{\rho V \sqrt{K}}{\mu} \tag{7}$$

$$f = \frac{(-dP/dx)\sqrt{K}}{\rho V^2} \tag{8}$$

The complete dataset is used to develop an empirical correlation f–Re_K relationship:

$$f = \frac{1}{\mathrm{Re}_K} + 0.105 \tag{9}$$

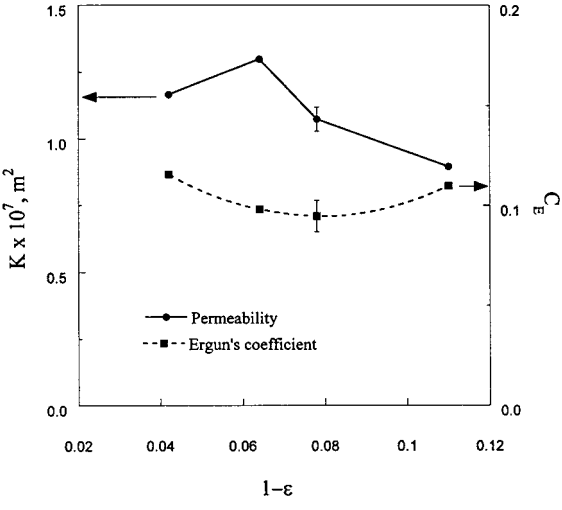

Fig. 10. Effect of porosity on permeability and Ergun's coefficient at a fixed cell size, $d = 1.25$ mm.

The information on Ergun's coefficient C_E has been embedded in the last constant in Eq. (9). It should be noted that the C_E value, which represents inertial effects, is sensitive to the roughness of the foam metal, which in turn strongly depends on the shape of the ligament and cell structure. The above formula is plotted in Fig. 11, together with other published results.

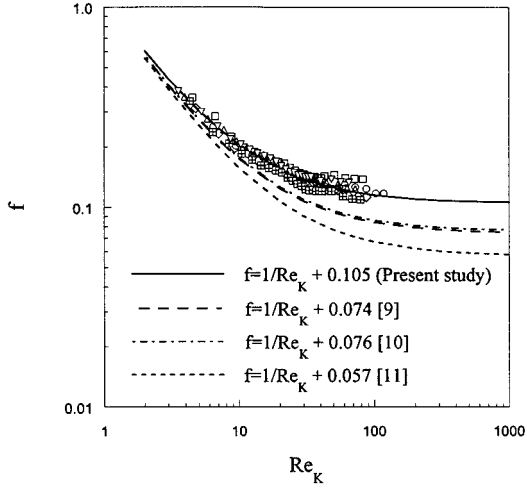

Fig. 11. Friction factor correlations.

The data of Beavers and Sparrow [9] and Hamaguchi et al. [10] are for nickel-based foam metals. As commented on by Takegoshi et al. [8], the specific manufacturing processes for aluminum- and nickel-based foam metals involve considerable differences which yield varying cell and ligament shapes and structures. These aspects are reflected in different values of C_E.

4. CONCLUSIONS

The thermophysical properties of aluminum-based foam metal, in particular, the effective thermal conductivity k_e and the permeability K, have been measured. It is found that k_e increases as the porosity ε decreases. However, k_e is little affected by variations in the cell size at fixed ε. The permeability is seen to be influenced appreciably by both the porosity and the cell size. By compiling the entire measurement data, a correlation for the friction factor $f = (\mathrm{Re}_K)^{-1} + 0.105$ is proposed which is qualitatively consistent with the previously published results.

ACKNOWLEDGMENTS

The authors acknowledge the financial support of MOST and Jang Han Eng., Inc., for this work and useful discussion with M. A. Beattie and B. D. Leyda at ERG, Inc.

REFERENCES

1. M. Sozen, K. Vafai, and L. A. Kennedy, *J. Thermophys. Heat Transfer* **5**:623 (1991).
2. F. W. Schmidt and A. J. Willmott, *Thermal Energy Storage and Regeneration* (McGraw-Hill, New York, 1981).
3. K. Ofuchi and D. Kunii, *Int. J. Heat Mass Transfer* **8**:749 (1965).
4. G. R. Hadley, *Int. J. Heat Mass Transfer* **29**:909 (1986).
5. M. L. Hunt and C. L. Tien, *Int. J. Heat Mass Transfer* **31**:301 (1988).
6. W. J. Mantle and W. S. Chang, *J. Thermophys. Heat Transfer* **5**:545 (1991).
7. T. H. Bauer, *Int. J. Heat Mass Transfer* **36**:4181 (1993).
8. E. Takegoshi, Y. Hirasawa, J. Matsuo, and K. Okui, *Trans. Jpn. Soc. Mech. Eng.* **58**(547B):879 (1992) [in Japanese].
9. G. S. Beavers and E. M. Sparrow, *J. Appl. Mech.* **36**:711 (1969).
10. K. Hamaguchi, S. Takahashi, and H. Miyabe, *Trans. Jpn. Soc. Mech. Eng.* **49**(445B):1991 (1983) [in Japanese].
11. K. Vafai and C. L. Tien, *Int. J. Heat Mass Transfer* **25**:1183 (1982).
12. G. N. Dul'nev, *J. Eng. Phys.* **9**:275 (1965).
13. M. Kaviany, *Principles of Heat Transfer in Porous Media* (Springer-Verlag, New York, 1991), pp. 42–46.